Serguei Yu. Maliassov* and Yuri V. Vassilevski

Extracting connectivity paths in digital core images using solution of partial minimum eigenvalue problem

https://doi.org/10.1515/rnam-2023-0028
Received October 23, 2023; accepted October 27, 2023

Abstract: We show theoretically and numerically that the lowest non-trivial eigenvector function for a specific eigenproblem has almost constant values in high conductivity channels, which are different in separate channels. Therefore, based on these distinct values, all separate connected clusters of open pores can be identified in digital cores.

Keywords: Eigenvalue problem, digital core, connectivity path.

MSC 2010: 65N25, 65Z05

Modelling rock properties based on digital core images plays an increasingly important role in the characterization of source rocks in oil and gas exploration. The accuracy of three-dimensional digital core reconstruction is extremely important for determining those properties. Usual resolutions of 3D X-Ray Micro-CT (XMCT) core images may amount to thousands of voxels in each direction resulting in billions of voxels in a single image. Direct numerical simulations of fluid flow through digitized core image using such voxsets represent real computational challenge even on advanced HPC systems.

Analysis of many digital core images reveals that not all open pores are connected. Extracting connected parts and modelling flows in each part separately may dramatically decrease the complexity of numerical simulation. Moreover, modelling separate connected parts simultaneously in parallel environment may further decrease the computational time.

A similar problem arises in multiscale finite element method [1] where there is a need to extract local highly permeable subvolumes.

Extraction of the connected subsets of voxels may seem analogous to the computation of connectivity paths in seismic volumes (see [8] and the references therein), but it has one obvious distinction. While the extraction of connectivity paths in seismic volumes is aimed to find the curves or surfaces along which the magnitude of some property (e.g., the amplitude of the impedance relative changes) is maximal, a search for the connected subsets of open pores in the core image may lead to sizeable 3D volumes. Thus, the algorithms for searching the subsets of lower dimension are not very useful for extraction volumetric subsets of voxels.

Another way to find the connected subsets of voxels can be based on the algorithms for solving connected component problem for undirected graph [4]. Computational cost for solving such problem for a graph with n nodes and m edges is proportional to $O(m \cdot \alpha(m, n))$, where $\alpha(m, n)$ is the functional inverse of Ackermann's function, which grows very rapidly with increasing m and n. Even though there is a parallel analogue of that algorithm [9] it has scaling limitations due to relatively high communication overhead.

A very different way to extract connected parts of voxels from very large voxsets is based on the idea expressed in [2] for construction of multiscale basis functions in the domains with high contrast regions. Following this approach, we considered the eigenvalue problem $-\operatorname{div}(K\nabla u) = \lambda K u$ with very high value of the coefficient K in the open voxels and very low value in the voxels filled with rock. Our expectation based on [3] was that

***Corresponding author: Serguei Yu. Maliassov,** Scientific Center for Information Technology and Artificial Intelligence, Sirius University of Science and Technology, Sochi 354340, Russia. E-mail: malyasov.sy@talantiuspeh.ru
Yuri V. Vassilevski, Marchuk Institute of Numerical Mathematics of the Russian Academy of Sciences, Moscow 119333, Russia; Scientific Center for Information Technology and Artificial Intelligence, Sirius University of Science and Technology, Sochi 354340, Russia

solving that eigenvalue problem with uniform Neumann boundary conditions for the eigenspace corresponding to the lowest non-trivial eigenvalue should give us the conductivity channels. The multiplicity of the lowest eigenvalue should be equal to the number of separate conductive channels.

In this short note, we provide our observation revealing a different result. In our experiments the multiplicity of the minimal non-trivial eigenvalue is one, the corresponding eigenvector function has almost constant values in high conductivity channels, which are different in separate channels. In other words, separate connected parts can be identified by separate values of eigenvector function corresponding to the minimal nonzero eigenvalue.

1 Numerical framework

We consider the eigenvalue problem in a parallelepiped $\Omega \subset \mathbb{R}^3$ [3]:

$$-\operatorname{div}(K\nabla u) = \lambda K u \tag{1.1}$$

with homogeneous Neumann boundary conditions. It is well known [7] that problem (1.1) has semipositive discrete spectrum with minimal eigenvalue equal to 0 with the constant eigenfunction.

We will seek for the eigenspace corresponding to the minimal non-trivial eigenvalue by minimizing the corresponding Rayleigh quotient

$$\frac{\int_\Omega K\,|\nabla\varphi|^2}{\int_\Omega K\,|\varphi|^2} \longrightarrow \min_{(\varphi,1)=0}. \tag{1.2}$$

Let $\mathcal{T}_h$ be a conformal rectangular partition of the domain Ω, with n_x, n_y, n_z elements in each direction, $\mathcal{T}_h = \bigcup c_{i,j,k}$, $i = 1,\dots,n_x$, $j = 1,\dots,n_y$, $k = 1,\dots,n_z$. Without loss of generality we can assume that mesh sizes in all three directions are constant and equal to h, and coefficient K is piecewise constant in Ω and K_{ijk} is constant in each cell of the mesh.

Using the finite volume approximation for (1.1) on the rectangular grid results in the following eigenvalue problem of size $N = n_x \times n_y \times n_z$:

$$A\mathbf{x} = \lambda B\mathbf{x} \tag{1.3}$$

with a symmetric semi-positive definite seven-diagonal matrix A and a diagonal matrix B.

The diagonal entries of matrix B have values

$$B_{ijk} = h^3 K_{ijk}.$$

The entries of matrix A have the following values

$$\begin{gathered}
A_{ijk;ijk} = h\left(T_{ijk,i-1jk} + T_{ijk,i+1jk} + T_{ijk,ij-1k} + T_{ijk,ij+1k} + T_{ijk,ijk-1} + T_{ijk,ijk+1}\right)\\
A_{ijk;i-1jk} = -hT_{ijk,i-1jk}, \qquad A_{ijk;i+1jk} = -hT_{ijk,i+1jk}, \qquad A_{ijk;ij-1k} = -hT_{ijk,ij-1k}\\
A_{ijk;ij+1k} = -hT_{ijk,ij+1k}, \qquad A_{ijk;ijk-1} = -hT_{ijk,ijk-1}, \qquad A_{ijk;ijk+1} = -hT_{ijk,ijk+1}
\end{gathered}$$

where

$$T_{ijk,\alpha\beta\gamma} = \frac{2\,K_{ijk}\,K_{\alpha\beta\gamma}}{K_{ijk} + K_{\alpha\beta\gamma}}$$

for internal elements $c_{i,j,k}$, $i = 2,\dots,n_x - 1$, $j = 2,\dots,n_y - 1$, $k = 2,\dots,n_z - 1$, with obvious modification for boundary elements. For example, for cells with indices $i = 1$, $j = 2,\dots,n_y - 1$, $k = 2,\dots,n_z - 1$, we have

$$A_{ijk;ijk} = h\left(T_{ijk,i+1jk} + T_{ijk,ij-1k} + T_{ijk,ij+1k} + T_{ijk,ijk-1} + T_{ijk,ijk+1}\right).$$

2 Analysis of the lowest non-trivial eigenvector

In what follows, we assume that the domain has several, say n_c, separate (non-connected) subsets of mesh cells corresponding to open voxels, where we set very high value of constant coefficient K_x. In all other mesh cells, i.e., voxels filled with rock, we set very small value of constant coefficient, K_n, such that

$$r = K_n/K_x \ll 1. \tag{2.1}$$

For simplicity of presentation we consider the case with $n_z = 1$ although all derivations and conclusions are valid for full 3D formulation.

Obviously, since we consider the Neumann problem (1.1), the lowest eigenvalue is 0, has multiplicity 1, and the corresponding eigenvector is constant. All the other eigenvalues will have corresponding eigenvectors orthogonal to the constant vector. For this reason we are to investigate the eigenvalue system (1.3) in the subspace orthogonal to a constant.

Let us introduce several notations. We denote the separate sets of cells corresponding to open voxels as C_s, $s = 1, \dots, n_c$, and the rest of the cells as a set C_0. Also, we denote the sets of faces between the cells corresponding to open voxels as B_s, $s = 1, \dots, n_c$, the sets of faces between the cells corresponding to open voxels and rock voxels as B_{gs}, $s = 1, \dots, n_c$, and the rest of internal faces as B_0. By a face f belonging to any of B_* we understand a pair of duplets $(ij, \alpha\beta)$ denoting two adjacent cells sharing that face.

Now, let us consider the minimization of discretized Rayleigh quotient in the subspace orthogonal to the constant

$$\frac{(A\mathbf{u}, \mathbf{u})}{(B\mathbf{u}, \mathbf{u})} \to \min_{(\mathbf{u},\mathbf{1})=0}. \tag{2.2}$$

Using introduced notation for cell sets we can rewrite the denominator in (2.2) as

$$(B\mathbf{u}, \mathbf{u}) = h^3 \sum_{s=1}^{n_c} \sum_{(i,j)\in C_s} K_x u_{i,j}^2 + h^3 \sum_{(i,j)\in C_0} K_n u_{i,j}^2. \tag{2.3}$$

The nominator in turn can be rewritten as

$$(A\mathbf{u}, \mathbf{u}) = h \sum_{s=1}^{n_c} \sum_{(ij,\alpha\beta)\in B_s} T_{ij,\alpha\beta}(u_{ij} - u_{\alpha\beta})^2 + h \sum_{s=1}^{n_c} \sum_{(ij,\alpha\beta)\in B_{gs}} T_{ij,\alpha\beta}(u_{ij} - u_{\alpha\beta})^2 + h \sum_{(ij,\alpha\beta)\in B_0} T_{ij,\alpha\beta}(u_{ij} - u_{\alpha\beta})^2. \tag{2.4}$$

Since for all faces from B_s, $s = 1, \dots, n_c$, we have

$$T_{ij,\alpha\beta} = \frac{2\,K_{ij}\,K_{\alpha\beta}}{K_{ij} + K_{\alpha\beta}} = K_x$$

for all faces from B_{gs}

$$T_{ij,\alpha\beta} = \frac{2\,K_{ij}\,K_{\alpha\beta}}{K_{ij} + K_{\alpha\beta}} = \frac{2K_n K_x}{K_n + K_x}$$

and for all faces from B_0

$$T_{ij,\alpha\beta} = \frac{2\,K_{ij}\,K_{\alpha\beta}}{K_{ij} + K_{\alpha\beta}} = K_n$$

we can rewrite (2.4) as follows

$$(A\mathbf{u}, \mathbf{u}) = h \sum_{s=1}^{n_c} \sum_{(ij,\alpha\beta)\in B_s} K_x(u_{ij} - u_{\alpha\beta})^2 + h \sum_{s=1}^{n_c} \sum_{(ij,\alpha\beta)\in B_{gs}} \frac{2K_n K_x}{K_n + K_x}(u_{ij} - u_{\alpha\beta})^2 + h \sum_{(ij,\alpha\beta)\in B_0} K_n(u_{ij} - u_{\alpha\beta})^2. \tag{2.5}$$

Using (2.1), (2.3), and (2.5) we can rewrite (2.2) as

$$\frac{hK_x \left(\sum\limits_{s=1}^{n_c} \left(\sum\limits_{(ij,\alpha\beta)\in B_s} (u_{ij} - u_{\alpha\beta})^2 + \frac{2r}{1+r} \sum\limits_{(ij,\alpha\beta)\in B_{gs}} (u_{ij} - u_{\alpha\beta})^2 \right) + r \sum\limits_{(ij,\alpha\beta)\in B_0} (u_{ij} - u_{\alpha\beta})^2 \right)}{h^3 K_x \left(\sum\limits_{s=1}^{n_c} \sum\limits_{(ij)\in C_s} u_{ij}^2 + r \sum\limits_{(ij)\in C_0} u_{ij}^2 \right)} \to \min_{(\mathbf{u},\mathbf{1})=0}.$$

Simplifying further we get

$$\frac{\sum\limits_{s=1}^{n_c}\left(\sum\limits_{(ij,\alpha\beta)\in B_s}(u_{ij}-u_{\alpha\beta})^2+\frac{2r}{1+r}\sum\limits_{(ij,\alpha\beta)\in B_{gs}}(u_{ij}-u_{\alpha\beta})^2\right)+r\sum\limits_{(ij,\alpha\beta)\in B_0}(u_{ij}-u_{\alpha\beta})^2}{h^2\left(\sum\limits_{s=1}^{n_c}\sum\limits_{(ij)\in C_s}u_{ij}^2+r\sum\limits_{(ij)\in C_0}u_{ij}^2\right)}\to\min_{(\mathbf{u},\mathbf{1})=0}. \tag{2.6}$$

If in the ratio (2.6) we take a limit as $r\to 0$ we get

$$\frac{\sum\limits_{s=1}^{n_c}\sum\limits_{(ij,\alpha\beta)\in B_s}(u_{ij}-u_{\alpha\beta})^2}{h^2\sum\limits_{s=1}^{n_c}\sum\limits_{(ij)\in C_s}u_{ij}^2}\to\min_{(\mathbf{u},\mathbf{1})=0}. \tag{2.7}$$

The minimum in (2.7) is achieved when in each set B_s the values of u_{ij} are the same, i.e., the vector is constant in each set. Since the global vector $\mathbf{u}$ should be orthogonal to $\mathbf{1}$, those constants can not be the same in each set. Thus, there is at least one set, say B_1, in which the values of the eigenvector u_{ij} are constant and different from the values in the other sets B_s, $s=2,\dots,n_c$. Our goal is to show that these constants should be different in each set.

For the case $n_c=2$ it is obvious. Let us consider the case $n_c>2$.

Assume for a moment that there are two sets, say B_1 and B_2, in which these constants coincide and in the rest of sets B_i, $i=3,\dots,n_c$, those constant values are different.

Using the inequality

$$\frac{a_1+a_2}{b_1+b_2}\leqslant\max\left\{\frac{a_1}{b_1},\frac{a_2}{b_2}\right\}$$

where $a_1\geqslant 0$, $a_2\geqslant 0$, $b_1>0$, $b_2>0$, we estimate from above the left part of (2.6) by

$$\begin{aligned}
&\frac{\sum\limits_{s=1}^{n_c}\left(\sum\limits_{(ij,\alpha\beta)\in B_s}(u_{ij}-u_{\alpha\beta})^2+\frac{2r}{1+r}\sum\limits_{(ij,\alpha\beta)\in B_{gs}}(u_{ij}-u_{\alpha\beta})^2\right)+r\sum\limits_{(ij,\alpha\beta)\in B_0}(u_{ij}-u_{\alpha\beta})^2}{h^2\left(\sum\limits_{s=1}^{n_c}\sum\limits_{(ij)\in C_s}u_{ij}^2+r\sum\limits_{(ij)\in C_0}u_{ij}^2\right)}\\
&\leqslant\max\left\{\frac{\sum\limits_{s=1}^{n_c}\sum\limits_{(ij,\alpha\beta)\in B_s}(u_{ij}-u_{\alpha\beta})^2+\frac{2r}{1+r}\sum\limits_{s=3}^{n_c}\sum\limits_{(ij,\alpha\beta)\in B_{gs}}(u_{ij}-u_{\alpha\beta})^2}{h^2\sum\limits_{s=1}^{n_c}\sum\limits_{(ij)\in C_s}u_{ij}^2},\right.\\
&\left.\frac{\sum\limits_{(ij,\alpha\beta)\in B_0}(u_{ij}-u_{\alpha\beta})^2+\frac{2}{1+r}\left(\sum\limits_{(ij,\alpha\beta)\in B_{g1}}(u_{ij}-u_{\alpha\beta})^2+\sum\limits_{(ij,\alpha\beta)\in B_{g2}}(u_{ij}-u_{\alpha\beta})^2\right)}{h^2\sum\limits_{(ij)\in C_0}u_{ij}^2}\right\}.
\end{aligned}\tag{2.8}$$

The first term in the right hand side of (2.8) when we take $r\to 0$ turns into

$$\frac{\sum\limits_{s=1}^{n_c}\sum\limits_{(ij,\alpha\beta)\in B_s}(u_{ij}-u_{\alpha\beta})^2}{h^2\sum\limits_{s=1}^{n_c}\sum\limits_{(ij)\in C_s}u_{ij}^2}$$

which vanishes as in all sets C_s, $s=1,\dots,n_c$, the values u_{ij} coincide with $u_{\alpha\beta}$.

The second term in the right hand side of (2.8) is bounded from above by

$$2\frac{\sum\limits_{(ij,\alpha\beta)\in B_0}(u_{ij}-u_{\alpha\beta})^2+\left(\sum\limits_{(ij,\alpha\beta)\in B_{g1}}(u_{ij}-u_{\alpha\beta})^2+\sum\limits_{(ij,\alpha\beta)\in B_{g2}}(u_{ij}-u_{\alpha\beta})^2\right)}{h^2\sum\limits_{(ij)\in C_0}u_{ij}^2}$$

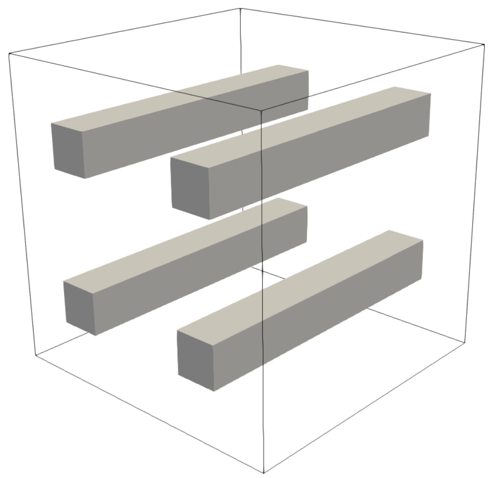

Fig. 1: The domain with 4 highly conductive beams.

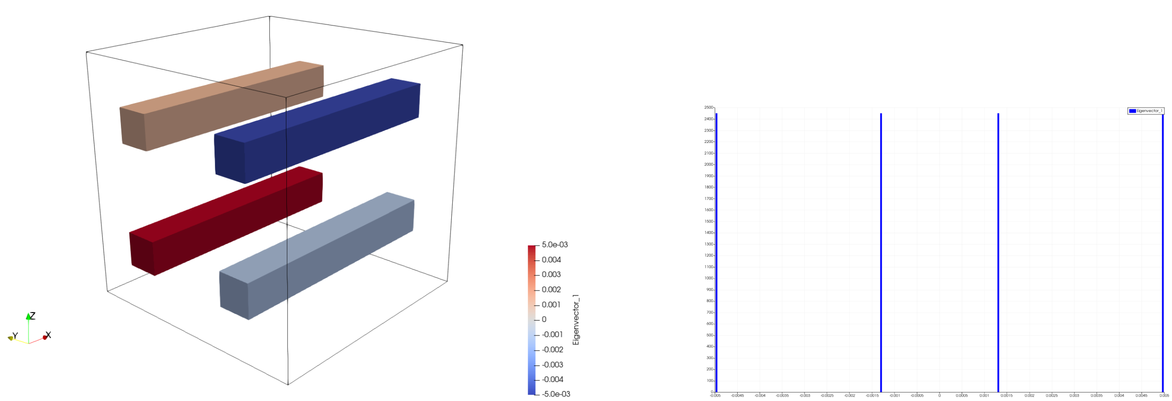

(a) The values of the eigenvector

(b) The histogram of the values

Fig. 2: The values of the lowest non-trivial eigenvector in 4 highly conductive beams.

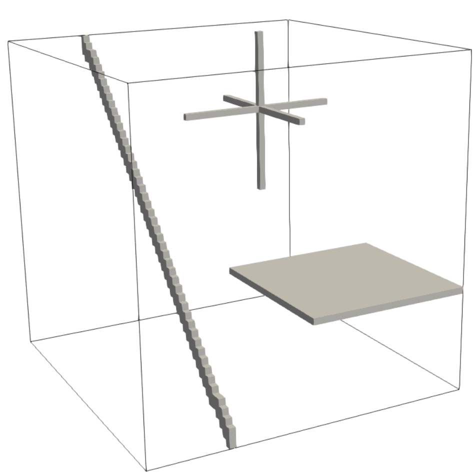

Fig. 3: The domain with 3 highly conductive regions.

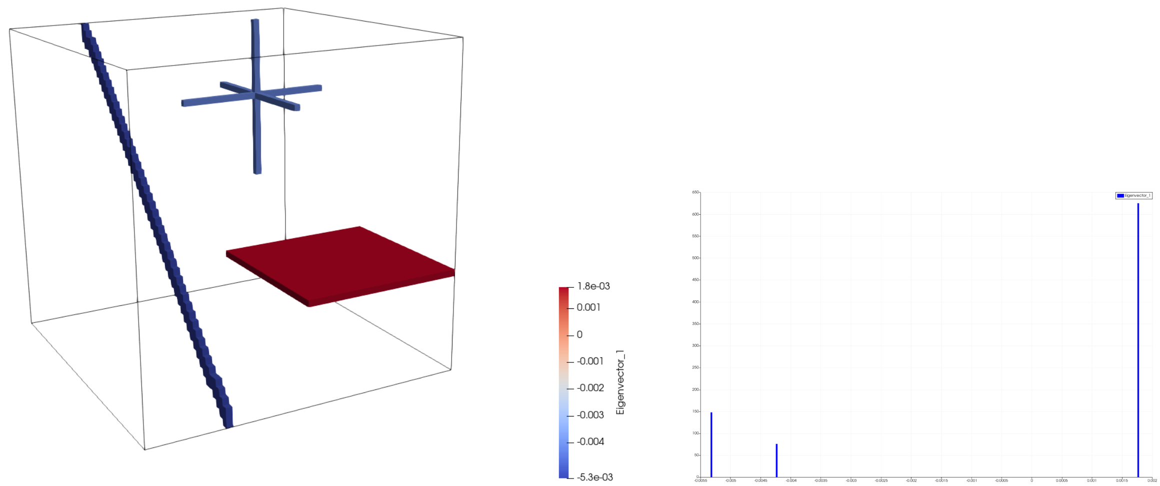

(a) The values of the eigenvector (b) The histogram of the values

Fig. 4: The values of the lowest non-trivial eigenvector in 3 highly conductive regions of different shapes.

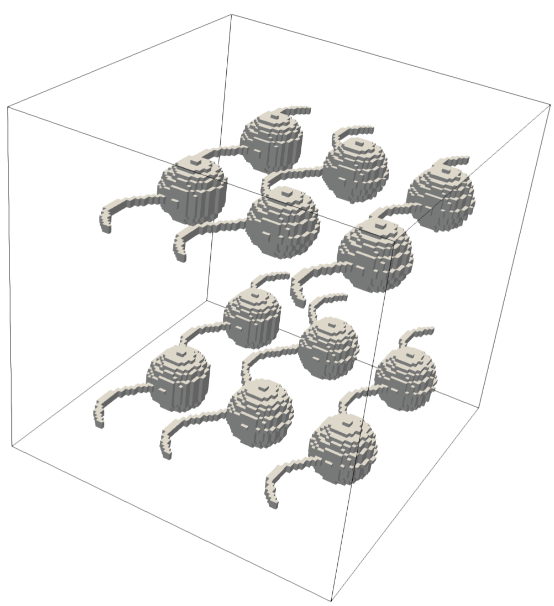

Fig. 5: The domain with multiple highly conductive spherical shapes connected by channels.

for any $0 \leqslant r \leqslant 1$. The latter ratio can be considered as the Rayleigh quotient for the problem

$$-\operatorname{div}(2\nabla v) = \lambda v$$

on a domain consisting of all cells from the set C_0 with Neumann boundary conditions on all the boundary faces except boundary faces adjacent to the sets of cells B_1 and B_2. In the latter boundary faces, the Dirichlet boundary conditions are imposed with the constant values corresponding to the constant values of the eigenvector u_{ij} in B_1 and B_2, respectively. Note that these constants coincide by the assumption. Now, if we connect any point on the boundary B_1 with any point on the boundary B_2 by a smooth curve belonging to the domain C_0, then by the Hopf's lemma (the maximum principle) the values of function v along that curve should be between the values on the boundaries B_1 and B_2 that is the value should be constant. That means that function v should be constant in all C_0 and the second term in (2.8) also should be zero.

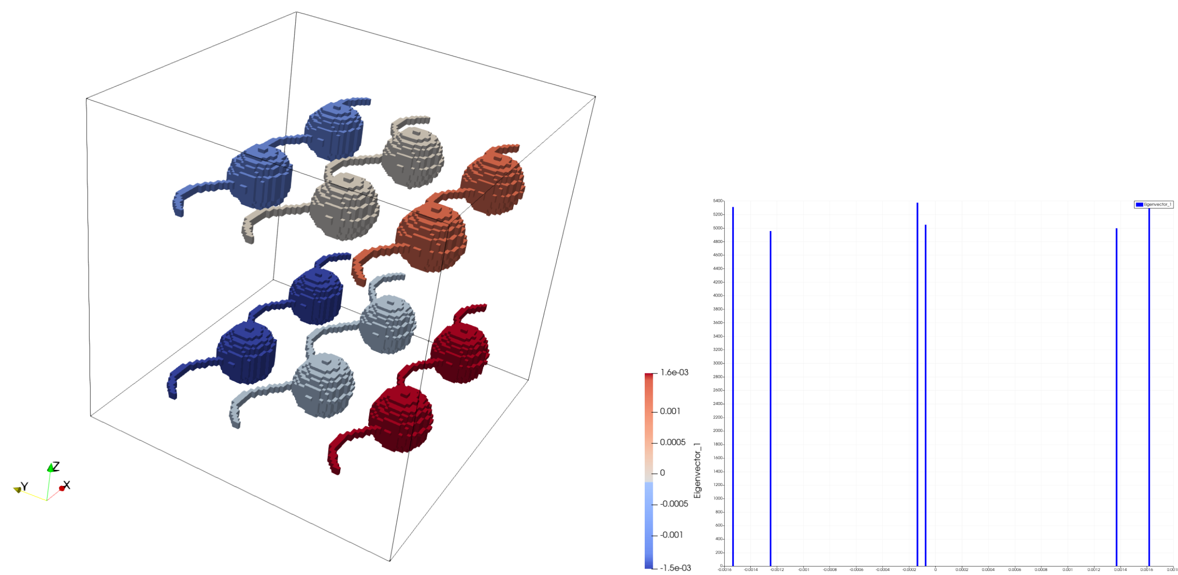

(a) The values of the eigenvector

(b) The histogram of the values

Fig. 6: The values of the lowest non-trivial eigenvector in multiple highly conductive spherical shapes.

Thus, we obtained the following. We got the vector **u**, which is constant in the subdomains C_0, B_1, and B_2, also in the other subdomains B_i, $i = 3, \dots, n_c$, the values of this vector are constants different than the value in the former subsets, this vector is orthogonal to **1**, and the Rayleigh quotient on it is equal to 0. In other words, there exists a vector **u** orthogonal to **1** for which Rayleigh quotient (2.6) becomes zero due to inequality (2.8) as we tend the ratio K_n/K_x to zero. That means the zero eigenvalue has multiplicity more than 1, and we have to admit the contradiction. Thus, there may not be any two sets B_i and B_j, which have the same value of constant for the lowest non-trivial eigenvector.

We have to note that the values of the lowest non-trivial eigenvector become constant in high conductivity regions as the ratio (2.1) tends to zero, $r \to 0$. For any small nonzero r we may expect that the values of the lowest non-trivial eigenvector in each separate highly conductive region will be close to a unique constant. This constant should be separated from the constants characterizing the other highly conductive regions.

This observation gives us a practical way to extract the separate regions of high conductivity in digital core images analyzing the first non-trivial eigenvector.

3 Numerical experiments

The goal of our experiments is to investigate numerically the behaviour of the lowest non-trivial eigenvector. To this end, we employ the block preconditioned conjugate gradient method [5] implemented in the framework of Hypre software [6]. We address the cubic mesh in the unit cube, $n_x = n_y = n_z = 100$, and different geometries of conductive regions with $K = 1$, the rest of the 3D domain is formed by regions with low conductivity $K = 10^{-9}$.

In the first experiment we consider four highly conductive beams along x-direction as shown in Fig. 1.

The values of the eigenvector corresponding to the first non-trivial eigenvalue in the highly conductive beams are shown in Fig. 2. The left picture shows the color coded values in the beams of high conductivity while the right picture shows the histogram for distribution of those values in the beams. The values of the eigenvector shown in Fig. 2 have distinct values in different beams, which fall into separate bins in histogram.

In the second experiment we consider three highly conductive regions of different shapes, namely a plane parallel to xy-plane, a 3D cross, and a slanted line shown in Fig. 3.

The values of the lowest non-trivial eigenvector in the zones of high conductivity are shown in the left picture of Fig. 4. The right picture of Fig. 4 represents distribution of those values, which proves their clusterization around three distinct values.

In the third experiment we generate multiple highly conductive spherical shapes connected by sinusoidal channels, see Fig. 5.

The values of the lowest non-trivial eigenvector in the zones of high conductivity are shown in the left picture of Fig. 6. The right picture of Fig. 6 represents distribution of those values, which proves their clusterization around distinct values.

4 Conclusions

The discovered property of the eigenvector corresponding to the lowest non-zero eigenvalue of problem (1.3) can be used to extract connected parts of open pores in the micro-CT image of a core in the following way. For a given voxset image one assigns high permeability coefficient to open pores and very low permeability coefficient to pores filled with rock. Then one computes the lowest non-trivial eigenvector of (1.3) and clusterizes values of that eigenvector corresponding to all open pores. The number of distinct clusters of these values will give the number of distinct channels of open pores. Each cluster extracts a separated channel from the whole set of open pores.

Acknowledgment: The authors would like to thank Dr. Yalchin Efendiev for fruitful discussions and valuable suggestions.

Funding: The work is supported by the Ministry of Science and Higher Education of the Russian Federation, Agreement 075-10-2021-093, Project MMD-RND-2265.

References

[1] E. T. Chung, Y. Efendiev, and W. T. Leung, Constraint energy minimizing generalized multiscale finite element method. *Computer Methods in Applied Mechanics and Engineering* **339** (2018) 298–319.

[2] Y. Efendiev, J. Galvis, and T. Y. Hou, Generalized multiscale finite element methods (gmsfem). *J. Comput. Phys.* **251** (2013) 116–135.

[3] Y. Efendiev and W. T. Leung, Multicontinuum homogenization and its relation to nonlocal multicontinuum theories. *J. Comput. Phys.* **474** (2023), 111761.

[4] W. R. Franklin, S. V. G. de Magalhaes, and E. N. Landis, Fast 3-D Euclidean connected components. In: *3rd ACM SIGSPATIAL International Workshop on Spatial Gems* (SpatialGems 2021), November 2, 2021 (Ed. J. Krumm), ACM, 2021.

[5] A. V. Knyazev, Preconditioned eigensolvers. In: *Templates for the Solution of Algebraic Eigenvalue Problems: A Practical Guide* (Eds. Z. Bai, J. Demmel, J. Dongarra, A. Ruhe, and H. van der Vorst), SIAM, Philadelphia, PA, 2000, pp. 352–368.

[6] I. Lashuk, M. Argentati, E. Ovtchinnikov, and A. Knyazev, *Preconditioned Eigensolver LOBPCG in hypre and PETSc*, Vol. 55. Springer, Berlin–Heidelberg, 2007, pp. 635–642.

[7] M. A. Shubin, *Pseudodifferential Operators and Spectral Theory*. Springer, 2001.

[8] P. Thore and A. Lucas, Extracting connectivity paths in 3d reservoir property: A pseudo skeletonization approach. *Computers and Geosciences* **171** (2023), 105262.

[9] Y. Zhang, A. Azad, and A. Buluc, Parallel algorithms for finding connected components using linear algebra. *J. Parallel and Distributed Computing* **144** (2020), 14–27.